Optical pulling of dielectric particles with non-paraxial Bessel beams through Pancharatnam-Berry metasurfaces

Xinyu Huang, Yaokun Shi, Jianing Qin, and Zhe Shen*
School of Electronic and Optical Engineering, Nanjing University of Science and Technology, Nanjing 210094, China

ABSTRACT

Tractor beams have received increasing attention. The generation of tractor beams is an important issue in practical applications. In this paper, Pancharatnam-Berry (PB) metasurfaces were designed to generate non-paraxial Bessel tractor beams. The optical pulling forces (OPFs) exerted on dielectric particles with specific radii on the axis of the non-paraxial Bessel beam were obtained. The presence of OPFs depended on the size of the particles, indicating the potential of the non-paraxial Bessel tractor beam for separating particles. Such a feature illustrated the possibility of selective optical manipulation and sorting. This setup of metasurface has good potential in such aspects as lab-on-a-chip.

Keywords: optical pulling force, non-paraxial Bessel beam, tractor beam, Pancharatnam-Berry metasurface

1. INTRODUCTION

Since Ashkin's seminal work on optical trapping in 1970 [1], optical manipulation has experienced a flourishing development. Besides the original "trapping [2, 3]", other manipulation forms, such as "pulling [4]", "spinning [5]" and "rotating [6]" have been developed. They have a wide range of application prospects in biosynthesis [7] and microstructure assembly [8] and so on. Among these forms of manipulation, the counter-intuitive "optical pulling" stands out [9-12]. Till now, a variety of ways to achieve optical pulling force (OPF) have been applied. These methods can be divided into two categories. The first category of methods relies on some special properties of the target and background to generate OPFs passively. OPFs depend on the target with exotic optical parameters [13] and structured material background [14, 15]. The other category "actively" generates OPFs through the properties of the beams themselves. For example, coherent beams with a certain angle between the propagation directions, such as Gaussian beams [16] or plane waves [12], can exert OPFs on the particles. Similar results can be obtained with a single structured beam, such as a solenoid beam [17, 18] or a non-paraxial Bessel beam [9, 19].

It is a typical method to achieve OPFs on target particles with a single non-paraxial Bessel beam. Bessel beams have been applied in the optical sorting before [20, 21]. Through selective optical trapping on diffraction rings of different orders, researchers separated particles of different sizes. In previous studies, it has also been reported that the OPFs provided by non-paraxial Bessel beams was related to the radii of the particles [22], which also enables optical sorting with the OPFs in non-paraxial Bessel beams. Hence, a facile and efficient method to generate non-paraxial Bessel beams is highly necessary.

Traditional methods to generate non-paraxial Bessel beams require special axicon lenses [23] or a spatial light modulator (SLM) [24]. To generate a structured Bessel beam, additional optical device should be added. These all lead to the complexity of the entire optical system. Metasurface devices alleviate these problems. Metasurfaces have the ability to flexibly adjust the phase locally, and can add additional phase gradients [25] or the phase of optical vortices [26] to the initial phase profile. Such devices have good prospects for miniaturization and integration.

In this paper, we designed Pancharatnam-Berry (PB) metasurfaces, and the effect of the metasurfaces to generate non-paraxial Bessel beams was verified. The beams were expected to exert anomalous OPFs on dielectric particles. We expected to study the influence of parameters such as particle radius on the OPFs on the basis of verifying the existence of the OPFs, and study the possibility of non-paraxial Bessel tractor beams for optical sorting.

* shenzhe@njust.edu.cn

SPIE-CLP Conference on Advanced Photonics 2022, edited by Xu Liu, Anatoly Zayats, Xiaocong Yuan, Proc. of SPIE Vol. 12601, 126010F
 · 0277-786X · doi: 10.1117/12.2667160

2. THE DESIGN OF THE METASURFACES

The PB metasurfaces in this paper are composed of titanium dioxide (TiO_2) cuboid nanofins with a refractive index of 2.42 on the silica substrate as Fig. 1(b) shows. Each nanofin acts as a half-wave plate, which changes the polarization angle of a linearly polarized incident beam, or the phase of the circularly polarized incident beam. As Fig. 1(c) shows, when the nanofin rotates by an angle of θ in the counterclockwise direction, the phases of the outgoing left or right-handed circularly polarized beam change by minus or plus 2θ, respectively. By rotating nanofins appropriate angles, the desired phase distribution can be obtained. The nanofins were arranged in rings, with a spacing of 370 nm between each circle, and a spacing of 350 nm between each nanofin on a circle.

To generate a non-paraxial Bessel beam, the phase distribution should meet:

$$\psi(x,y)=\frac{2\pi}{\lambda}\sqrt{x^2+y^2}\sin\beta+m\arctan(\frac{y}{x}), \tag{1}$$

where (x, y) are the Cartesian coordinate of an arbitrary location on the metasurface. Parameter λ is the wavelength of the incident beam, m is the topological charge of the Bessel beam, and β is the half cone angle of the non-paraxial Bessel beam. According to Eq. 1, the rotation angle of the nanofins can be written as:

$$\theta(x,y)=u\left(\frac{\pi}{\lambda}\sqrt{x^2+y^2}\sin\beta+\frac{1}{2}\cdot m\arctan(\frac{y}{x})\right), \tag{2}$$

where u is a parameter related to beam polarization. For a left-handed circularly polarized (*l-circ-pol*) beam, $u=-1$, and for a right-handed circularly polarized (*r-circ-pol*) beam, $u=1$.

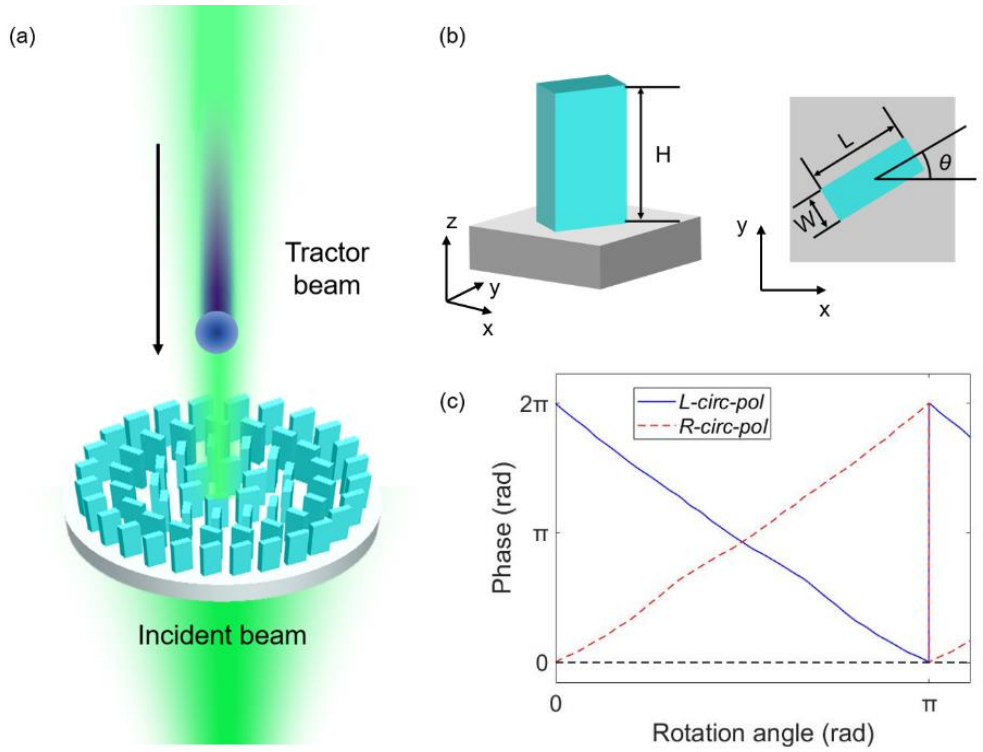

Fig. 1 (a) The schematic diagram of the generation of non-paraxial Bessel beams with the PB metasurface. (b) The schematic diagram of the cuboid nanofin. H = 600 nm, L = 250 nm, and W = 95 nm. (c) Changes in the phase of incident left and right-handed circularly polarized light when the nanofin is rotated.

3. SIMULATIONS WITH THE METASURFACES

In this section, in order to study the features of the optical forces in the non-paraxial Bessel beams on particles, we generated the beams with the metasurfaces designed above, and calculated the optical force exerted on the target particles in the simulations in vacuum with the finite difference time domain (FDTD) method. The radius of the metasurfaces were 10 μm. Incident beams were plane waves with left or right-handed circular polarization (*l-circ-pol* and *r-circ-pol* beams). The power of the incident beams was 0.01 W. The dielectric particles were polystyrene spheres with the refractive index of 1.55. The radius of the particle was expressed in *kr* (*k* is the wave number of the non-paraxial Bessel beam, and *r* is the radius of the sphere particle). We specified that the pulling force of the particles towards the light source is negative, and the pushing force is positive.

With the PB metasurfaces, incident plane waves with left and right-handed circular polarizations were employed in the simulations. Figs. 2(a) and (c) show the *x-z* cross-sectional views of the normalized intensity distributions of the non-paraxial Bessel beams with the two incident beams. The beams generated with the small-sized metasurfaces were satisfactory. In the following simulations to calculate the optical forces, the particles were located at the optical axis of $z = 2$ μm, where the intensity of the beam was at its maximum. Optical forces on particles with radii from $kr = 0.4$ to $kr = 4$ at the optical axis were calculated. It can be seen from Figs. 2(b) and (d) that the OPFs on particles in a non-paraxial Bessel beam were selective, and OPFs were exerted on the sphere particles with radii around $kr = 2$ with both the two incident beams, and the trend of the optical forces changing with the particle radius is almost the same. The differences between the two cases were within the error range. It is because the only difference between the two beams was the rotation of the polarization, and the target particle was a uniform sphere. Such a kind of non-paraxial Bessel beam can be regarded as a tractor beam, and the exit of OPFs depended on the radii of the particles. Particles with radii around $kr = 2$ were pulled towards the source, while particles with other radii were pushed away. Such a feature provides a possible of sorting nanoparticles based on their sizes employing the non-paraxial Bessel tactor beam.

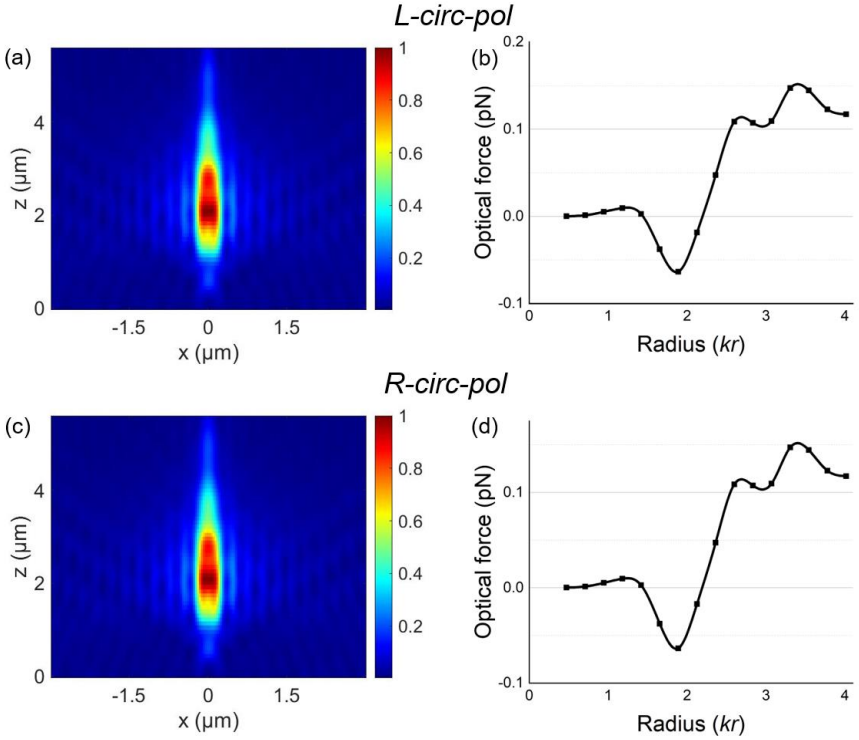

Fig. 2 (a) and (b) The non-paraxial Bessel beam generated with the PB metasurface with incident beams of left and right-handed circular polarization, resp5ectively. (c) and (d) Optical forces as a function of particle radii for two incident beams.

4. CONCLUSIONS

In this paper, PB metasurfaces were designed to generate non-paraxial Bessel tractor beam with the incident *l-circ-pol* and *r-circ-pol* beams. The metasurfaces generated desired beams satisfactorily with the two incident beams, and the tractor beams exerted OPFs on dielectric particles without the aid of the background or the exotic optical parameters of particles. The exit of OPFs depends on the radius of the target particles, and such a feature indicates the possibility of the non-paraxial Bessel beam for optical sorting based on the sizes of particles. Hence, our work has a potential application in optical particle manipulation and sorting, and this setup of metasurface has good potential in such aspects as lab-on-a-chip.

ACKNOWLEDGEMENTS

This work was supported by National Natural Science Foundation of China (61805119), Natural Science Foundation of Jiangsu Province (BK20180469; BK20180468), and Fundamental Research Funds for the Central Universities (30919011275).

REFERENCES

[1] A. Ashkin, "Acceleration and trapping of particles by radiation pressure," Physical Review Letters, 24(4), 156-159 (1970).
[2] D. G. Grier, "A revolution in optical manipulation," Nature, 424(6950), 810-816 (2003).
[3] A. Ashkin, [Optical trapping and manipulation of neutral particles using lasers] World Scientific, Hackensack, NJ (2006).
[4] A. Dogariu, S. Sukhov, and J. Sáenz, "Optically induced 'negative forces'," Nature Photonics, 7(1), 24-27 (2012).
[5] J. Ahn, Z. J. Xu, J. Bang et al., "Optically levitated nanodumbbell torsion balance and GHz nanomechanical rotor," Physical Review Letters, 121, 033603 (2018).
[6] Z. Shen, Z. Y. Xiang, Z. Y. Wang et al., "Optical spanner for nanoparticle rotation with focused optical vortex generated through a Pancharatnam-Berry phase metalens," Applied Optics, 60(16), 4820-4826 (2021).
[7] M. Koch, and A. Rohrbach, "Object-adapted optical trapping and shape-tracking of energy-switching helical bacteria," Nature Photonics, 6(10), 680-686 (2012).
[8] M. Righini, G. Volpe, C. Girard et al., "Surface plasmon optical tweezers: Tunable optical manipulation in the femtonewton range," Physical Review Letters, 100, 186804 (2008).
[9] J. Chen, J. Ng, Z. Lin et al., "Optical pulling force," Nature Photonics, 5(9), 531-534 (2011).
[10] K. Ding, J. Ng, L. Zhou et al., "Realization of optical pulling forces using chirality," Physical Review A, 89, 063825 (2014).
[11] A. Novitsky, W. Q. Ding, M. Y. Wang et al., "Pulling cylindrical particles using a soft-nonparaxial tractor beam," Scientific Reports, 7, 652 (2017).
[12] S. Sukhov, and A. Dogariu, "Negative nonconservative forces: optical 'tractor beams' for arbitrary objects," Physical Review Letters, 107, 203602 (2011).
[13] A. Mizrahi, and Y. Fainman, "Negative radiation pressure on gain medium structures," Optics Letters, 35(20), 3405-3407 (2010).
[14] V. Kajorndejnukul, W. Ding, S. Sukhov et al., "Linear momentum increase and negative optical forces at dielectric interface," Nature Photonics, 7(10), 787-790 (2013).
[15] M. I. Petrov, S. V. Sukhov, A. A. Bogdanov et al., "Surface plasmon polariton assisted optical pulling force," Laser & Photonics Reviews, 10(1), 116-122 (2016).
[16] O. Brzobohaty, V. Karasek, M. Siler et al., "Experimental demonstration of optical transport, sorting and self-arrangement using a 'tractor beam'," Nature Photonics, 7(2), 123-127 (2013).
[17] S. H. Lee, Y. Roichman, and D. G. Grier, "Optical solenoid beams," Optics Express, 18(7), 6988-6993 (2010).
[18] L. Carretero, P. Acebal, C. Garcia et al., "Helical tractor beam: analytical solution of Rayleigh particle dynamics," Optics Express, 23(16), 20529-20539 (2015).

[19] A. Novitsky, C. W. Qiu, and H. F. Wang, “Single gradientless light beam drags particles as tractor beams,” Physical Review Letters, 107, 203601 (2011).
[20] L. Paterson, E. Papagiakoumou, G. Milne et al., “Light-induced cell separation in a tailored optical landscape,” Applied Physics Letters, 87, 123901 (2005).
[21] L. Paterson, E. Papagiakoumou, G. Milne et al., “Passive optical separation within a 'nondiffracting' light beam,” Journal of Biomedical Optics, 12(5), 054017 (2007).
[22] F. G. Mitri, R. X. Li, L. X. Guo et al., “Optical tractor Bessel polarized beams,” Journal of Quantitative Spectroscopy and Radiative Transfer, 187, 97-115 (2017).
[23] Z. Xie, V. Armbruster, and T. Grosjean, “Axicon on a gradient index lens (AXIGRIN): integrated optical bench for Bessel beam generation from a point-like source,” Applied Optics, 53(26), 6103-7 (2014).
[24] R. Bowman, N. Muller, X. Zambrana-Puyalto et al., “Efficient generation of Bessel beam arrays by means of an SLM,” European Physical Journal-Special Topics, 199(1), 159-166 (2011).
[25] Z. Shen, H. C. Liu, S. Zhang et al., “Optical manipulation of Rayleigh particles by metalenses-a numerical study,” Applied Optics, 58(21), 5794-5799 (2019).
[26] Z. Y. Xiang, Z. Shen, and Y. C. Shen, “Quasi-perfect vortices generated by Pancharatnam-Berry phase metasurfaces for optical spanners and OAM communication,” Scientific Reports, 12(1), 1053 (2022).